Thermochimica Acta 494 (2009) 115–122

Contents lists available at ScienceDirect

Thermochimica Acta

journal homepage: www.elsevier.com/locate/tca

Thermal degradation of carboxymethylcellulose in different salty forms

Douglas de Britto*, Odílio B.G. Assis

Embrapa Instrumentação Agropecuária, Rua XV de Novembro 1452, C.P. 741, 13560-970 São Carlos, SP, Brazil

ARTICLE INFO

Article history:
Received 15 January 2009
Received in revised form 18 March 2009
Accepted 30 April 2009
Available online 15 May 2009

Keywords:
Carboxymethylcellulose
Kinetic analysis
Thermal degradation

ABSTRACT

Carboxymethylcellulose (CMC) salts in different counter-ion forms were obtained and characterized by FTIR, CP-MAS ^{13}C NMR and EDX spectroscopies. Additionally, thermogravimetry (TG) was used to evaluate the degree of humidity and the thermal stability. In general, CMC samples having Li^+, Na^+ and K^+ as counter-ions showed a high hydrophilic character, absorbing more than 50% in weight of water, while for CMC having Mg^{2+}, Ca^{2+}, Ba^{2+} and others cations the hydrophilic character was lower than the former, absorbing less than 30% of water. All of the CMC salts showed lower thermal stability than their cellulose parent. Typical values of T_m, in °C, and E_a, in kJ mol^{-1}, were for cellulose: $T_m = 349.11$, $E_a = 178.8 \pm 8.4$; CMCK: $T_m = 283.61$, $E_a = 152.9 \pm 1.0$ kJ mol^{-1}; CMCCa: $T_m = 305.67$, $E_a = 167.2 \pm 5.2$ kJ mol^{-1}. Different kinetic models were found for the CMC salts as Šesták–Berggren, reaction order and Johnson–Mehl–Avrami.

1. Introduction

The chemical modification of polysaccharides is the most important route to change the properties of the naturally occurring biopolymers and to place this renewable resource in the context of sustainable development. Carboxymethylation is one of the most widely studied routes [1] since it is simple and leads to products with a variety of promising properties [2]. Carboxymethylation of cellulose yields the well known carboxymethylcellulose (CMC) that is extensively used in the food industry. The EU Food Standard Agency has approved CMC as an additive [3], labeled as E466 in the emulsifiers, stabilizers, thickeners and gelling agents category. But CMC has many other uses besides food additives and products such as toothpaste, laxatives, diet pills, ice cream, water-based paints, detergents, soap powder, and a variety of paper-based products may contain CMC [4,5].

CMC is mostly used in aqueous solutions [6], where useful characteristics such as high viscosity at low concentrations, defoaming, surfactant, and bulking abilities are applicable. However, in the solid-state CMC also has considerable applications, mainly as film, paints and paper products. In this condition, CMC may be associated with other ions that will influence its physical–chemistry properties. In the literature, studies related to the interaction of the carboxylic group with different metal cations are limited to aqueous solution in which works with calcium [7,8], copper [1 and references cited therein], lithium [2,9] and aluminum [10] have been reported. Thus, to obtain better comprehension of the CMC properties in the solid-state, this present work proposes to study CMC salts bearing different counter-ions concerning its water absorbance capacity and thermal stability as investigated by TG analysis.

2. Experimental

2.1. Synthesis of carboxymethylcellulose

The synthesis of CMC was carried out by a heterogeneous reaction in isopropyl alcohol, as an adapted sequence from the previously reported methodology [11], where ethanol was substituted by isopropyl alcohol. For this, 34 g of an aqueous solution of NaOH (40%) was slowly added under magnetic stirring to a suspension of 130 ml of isopropyl alcohol and 5 g of cellulose (obtained from bleached soda/anthraquinone pulp of sugar cane bagasse [12]). Next, 24 g of a solution of monochloroacetic acid in isopropyl alcohol (1:1) was added and the temperature was raised to 55 °C for 3.5 h. The raw CMC was isolated by filtration followed by neutralization with acetic acid. The CMC was purified by dissolution in an aqueous 0.2 M NaCl solution, followed by filtration to remove insoluble residues and recovered by precipitation with ethanol. Finally, the purified CMC was washed with acetone and dried at room temperature.

2.2. Counter-ions exchange

To obtain CMC in different salty forms, an aqueous solution at 1% CMC concentration was prepared and submitted to dialysis in a cellophane membrane (cut-off 12,000–14,000 g mol^{-1} from

* Corresponding author. Tel.: +55 16 21072800; fax: +55 16 21072902.
E-mail addresses: britto@cnpdia.embrapa.br (D. de Britto), odilio@cnpdia.embrapa.br (O.B.G. Assis).

0040-6031/$ – see front matter © 2009 Elsevier B.V. All rights reserved.
doi:10.1016/j.tca.2009.04.028

Aldrich) for 3 days against the aqueous 0.1 M solution of the desired cation. The salt used for this was: LiCl, KCl, $CaCl_2$, $MgCl_2$, $BaCl_2$, $AlCl_3$, $CuSO_4{\cdot}5H_2O$, $Fe_2(SO_4)_3{\cdot}nH_2O$ and $ZnSO_4{\cdot}7H_2O$ of chemical grade purchased from Mallinckrodt, Carlo Erba and Aldrich. The final products were obtained by precipitation with acetone. After exhaustive rinsing, the derivatives were filtered and dried at room temperature. The CMC was named according to its respective counter-ion, e.g., CMCNa, CMCLi, etc.

2.3. Characterization of CMC

CMC was characterized by infrared transformed Fourier (FTIR), solid-state CP-MAS ^{13}C NMR and energy dispersive X-ray (EDX) spectroscopies.

KBr pellets were prepared from each sample and the FTIR analysis was carried out in a PerkinElmer spectrometer (model Paragon 1000). Additionally, FTIR spectroscopy was used to study the chemical changes during the thermal degradation. For these, cast thin films of CMCNa were placed in an oven at 220 °C for different periods of time and the sample was directly analyzed in the FTIR spectrometer.

The solid-state CP-MAS ^{13}C NMR experiments were performed on a Varian Unity Inova 400 spectrometer operating at 400 MHz and ^1H frequency, using the combined techniques of proton dipolar decoupling (DD), magic angle spinning (MAS) and cross-polarization (CP). Contact time was 1 ms, acquisition time 51.2 ms and the recycle delay 4 s. The proton pulse width was 6 ms and an 18 kHz spectral window was used. Typically 2000 scans were acquired for each spectrum. The chemical shifts were externally referenced by setting the methyl resonance of hexamethylbenzene (HMB) to 17.3 ppm. The samples were contained in a SiN_4 cylindrical rotor which was spun at 5 kHz during measurements.

EDX analyses were conducted in a 440 Zeiss-Leika scanning electronic microscopy (SEM) equipment, equipped with a silicon(lithium) detector window (7060 Oxford EDX) with a resolution of 133 eV. The intensity of applied bundle of electrons was 20 keV. The analysis was performed in three different points of the surface sample.

2.4. Thermal analysis and kinetic study

The degree of humidity, non-isothermal and isothermal degradation studies were carried out using 7 mg of CMC in nitrogen atmosphere (gas flow of 60 ml min^{-1}) in a TGA500 from TA instruments.

The degree of humidity was determined in triplicate assays by heating the sample up to 150 °C and holding the isotherm for 20 min. Before the analysis the samples were conditioned in a chamber with 100% degree of humidity for 1 week.

For the non-isothermal experiments the samples were heated from room temperature to 500 °C at a heating rate varying from 2.5 to 15.0 °C min^{-1}. For the isothermal experiments the samples were heated at a rate of 10 °C min^{-1} to 150 °C, maintained at this temperature for 10 min and then equilibrated to the desired temperature for 80 min.

3. Results and discussion

3.1. Spectral characterization of CMC

The introduction of the $-CH_2COO^-Na^+$ group into the hydroxyl of the cellulose causes change in the pattern of the cellulose's FTIR basic spectrum (Fig. 1) due to the absorption of the carboxylate anion (COO^-). One of this absorption bands occurs at 1595 cm^{-1} (asymmetrical axial deformation) and another at 1417 cm^{-1} (symmetrical axial deformation). Others bands at

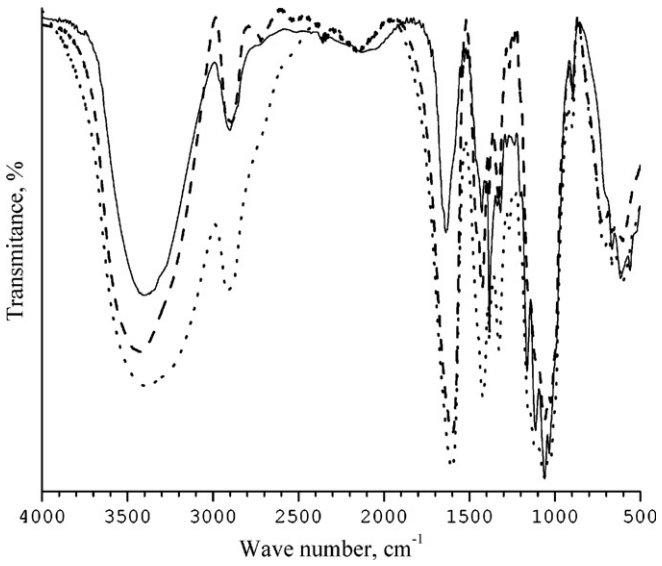

Fig. 1. FTIR spectra of the cellulose (—); CMCCa (- - -); CMCNa (…).

~3400 cm^{-1} (axial deformation of OH); ~2900 cm^{-1} (axial deformation of CH, CH_2); 1380–1300 cm^{-1} (angular deformation on the plane of OH); 1200–1000 cm^{-1} (axial deformation of CO, COC) are characteristics of gluco-polysaccharides and have been previously described in the literature [11,13]. Different counter-ions did not influence the position or intensity of the bands referent to carboxylate anion, as shown in Fig. 1 for CMCNa and CMCCa spectra.

EDX spectroscopy is a valuable tool to confirm the presence of the counter-ion in the CMC chain and to attest the purity of the sample. Fig. 2 shows typical EDX spectra for CMC salts, where it is possible to verify the signal of each cation serving as counter-ion. As reported in the literature [14], the main X-rays properties for edge energies in keV are $K\alpha = 1.04$ for Na; $K\alpha = 3.31$, $K\beta = 3.59$ for K; $K\alpha = 1.25$, $K\beta = 1.30$ for Mg; $K\alpha = 3.69$, $K\beta = 4.10$ for Ca; $L\alpha = 4.47$, $L\beta = 4.83$ for Ba; $K\alpha = 1.49$, $K\beta = 1.55$ for Al; $K\alpha = 8.05$, $K\beta = 8.90$ for Cu. It is noticeable that all of the X-ray lines from the EDX spectra (Fig. 2) match very well with those from literature for each cation.

EDX spectroscopy can be used as a quantitative tool for elemental analysis (Table 1). The experimental values agree fairly well with the calculated ones for samples CMCNa, CMCK, CMCMg, CMCCa and CMCAl, mainly for the counter-ion values. For the other samples the experimental values are, generally, superior to the theoretically calculated one. This is probably due to a non-stoichiometric relationship between the carboxylate anion and the divalent or trivalent cations. The predominant structure adopted by the glycoside ring is a relatively strain-free chair conformation. This conformation releases the steric hindrance but difficult polyvalent cations to binding stoichiometrically in all of the carboxylate groups. Thus, unsubstituted hydroxyl groups, inter and intra chain interaction and small anion, e.g., Cl^- or SO_4^{2-}, play an important role in the cation stabilization.

In the CP-MAS ^{13}C NMR spectra of cellulose and CMCNa (Fig. 3) the following main signals can be identified [2,15–17]: $\delta = 60$–70 ppm assigned to C6; a cluster of resonance centered at $\delta = 70$–81 ppm from C2, C3 and C5; the next region $\delta = 81$–93 ppm correspond to carbon atom C4, and finally for $\delta = 106$–108 ppm is assigned to carbon atom C1. The carboxyl group generates two signals referent to methylenic carbon (C7) at $\delta = 74$–77 ppm and another at $\delta = 179$–181 ppm due to the carbonylic carbon (C8). From the CMCNa spectrum the degree of substitution was calculated [2] as DS = 0.43.

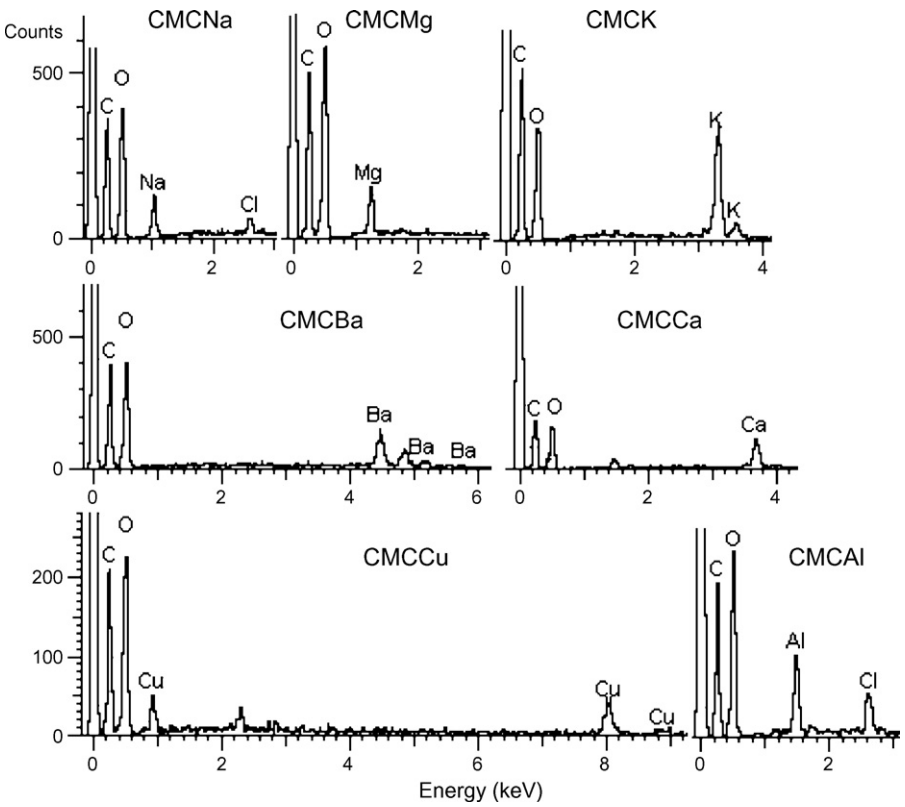

Fig. 2. Typical EDX spectra for CMC in different counter-ion forms.

3.2. Degree of humidity

Hydration has a significant influence on the physical properties of carbohydrates that reflect on its direct applications as cosmetics, anti-freezing properties in food, or protective film abilities. Several mechanisms have been proposed for moisture absorption by carbohydrates [18–20], however, in this present work the discussion is limited to the total sorbed water measured by TG analysis. The degree of humidity found for cellulose in a 100% relative humidity ambient was 13.6 ± 1.0, which is very close to that reported for cotton [18] and amorphous cellulose [20]. For the CMC salts with cations from alkali metal groups, the following humidity degree percentage was found: CMCLi = 43.1 ± 1.0; CMCNa = 71.0 ± 0.4; CMCK = 54.0 ± 4.0. According to previously reported data [18], the nature of the counter-ion is probably also important as the electrostatic field decreases. For alkali metals, the sequence of electrostatic field intensity is

Table 1
Elemental composition for CMC as found by EDX.

Sample	MW[a] (g mol^{-1})	Elemental composition (%)			
		C	O	Counter-ion	Others
CMCNa	195.40	43.74	49.59	6.67	–
		42.1 ± 5.1	51.1 ± 4.3	5.8 ± 1.6	0.9 ± 0.7[b]
CMCK	202.32	42.24	47.89	9.86	–
		38.8 ± 0.9	48.4 ± 0.5	12.9 ± 0.6	–
CMCMg	190.74	44.81	50.80	4.39	–
		33.5 ± 2.1	61.5 ± 2.7	5.0 ± 0.6	–
CMCCa	194.13	44.03	49.92	6.06	–
		44.6 ± 3.2	49.6 ± 4.1	5.7 ± 0.9	–
CMCBa	215.04	39.74	45.06	15.19	–
		39.4 ± 1.0	40.2 ± 4.0	20.4 ± 3.0	–
CMCAl	189.37	45.13	51.17	3.70	–
		47.7 ± 4.0	45.7 ± 3.1	3.9 ± 0.6	2.7 ± 0.5[b]
CMCFe	193.51	44.16	50.08	5.76	–
		44.2 ± 2.0	40.3 ± 2.7	11.6 ± 1.1	3.8 ± 0.4[c]
CMCCu	199.17	42.91	48.65	8.44	–
		45.2 ± 2.9	40.6 ± 2.5	14.2 ± 2.4	–
CMCZn	199.56	42.82	48.56	8.62	–
		45.1 ± 2.2	41.9 ± 3.3	13.1 ± 1.2	–

For each sample, the first line corresponds to theoretically calculated values and the second line corresponds to the experimental.

[a] The molecular weight was calculated assuming a DS = 0.43, as found by ^{13}C NMR, and an stoichiometry relationship between the carboxylate anion and the divalent or trivalent cations.

[b] Correspondent to Cl detected at 2.61 keV.

[c] Correspondent to S detected at 2.25 keV.

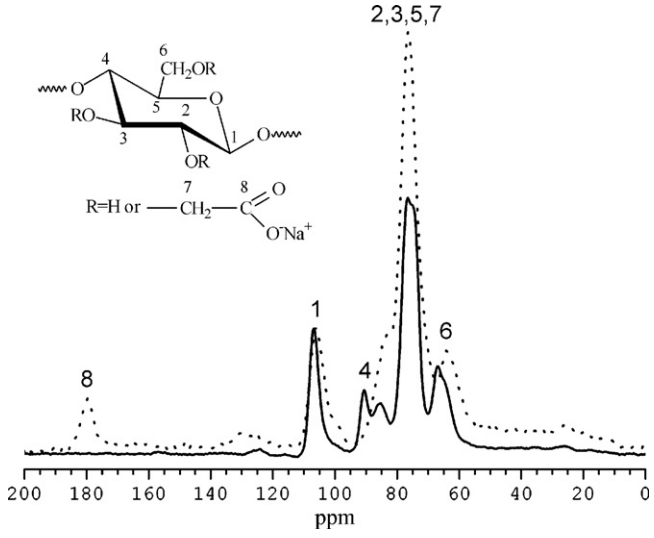

Fig. 3. CP-MAS ^{13}C NMR spectra of cellulose (—) and CMCNa (…).

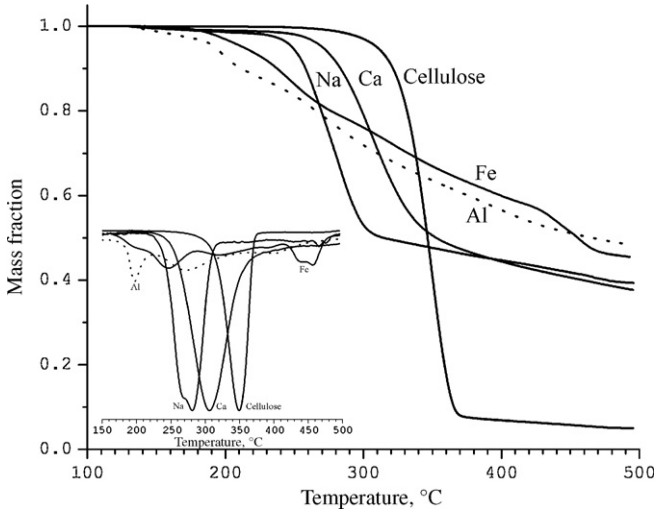

Fig. 4. Representative TG curves over the range of 100–500 °C in nitrogen atmosphere for cellulose, CMCNa, CMCCa, CMCAl and CMCFe at a heating rate of $\beta = 10.0\,^{\circ}\mathrm{C\,min^{-1}}$. Insert: corresponding DTG curves in an arbitrary scale for the range of 150–400 °C.

$Li^+ > Na^+ > K^+ > Rb^+ > Cs^+$, consequently the water uptake must follow the same order once the more pronounced the field, the stronger the effect on the surrounding water molecules. CMCNa and CMCK look to obey this rule but the CMCLi does not. It is known, however, that a stronger electrostatic field increases the intra molecular forces between side polysaccharide chains, resulting in a compact structure that reduces the water interaction. This is true for CMC in the acid form (non-dissociated –COOH groups) that results in an insoluble material due to the increase of intra chains hydrogen bonds. This phenomenon can explain the low degree of humidity found for CMCLi. This situation was not considered or detected in a previous study [18], where the following degrees of humidity were found for CMC (DS = 0.65): CMCLi = 60%; CMCNa = 55%; CMCK = 47%.

For the alkaline earth metals, the electrostatic field intensity appears to be directly responsible for the values of the degree of humidity that were: CMCMg = 31.5 ± 2.5; CMCCa = 29.0 ± 0.8; CMCBa = 25.0 ± 2.5. It is clear that the CMC with counter-ions of the alkaline earth metals presents lower affinity to water than the CMC with alkali metal cations. This was reported before [19] and a 38% degree of humidity was found for CMCCa [18].

Finally, for the other studied cations the following values for the degree of humidity were: CMCAl = 32.0 ± 2.0; CMCFe = 29.6 ± 0.5; CMCCu = 25.6 ± 0.5; CMCZn = 31.0 ± 1.4. These CMC salts showed low affinity to water and were slightly soluble.

3.3. General characteristics of the TG curves of the cellulose and CMC

The gases generated by the pyrolysis of cellulose consist mainly of H_2, CO_2, CO, CH_4, C_2H_6, C_2H_4, trace amounts of larger gaseous organics and water vapor [21]. This is an extremely complex process, generally undergoing a series of reactions [22]. The simplest feature of this process is the DTG peak temperature, corresponding to the maximum reaction rate, T_m, and the weight loss value. The TG curves for cellulose and some CMC, salts scanned at heating rate $\beta = 10\,^{\circ}\mathrm{C\,min^{-1}}$ over the range 100–500 °C, in nitrogen atmosphere, are shown in Fig. 4, while the corresponding DTG curves are depicted in the insert. For cellulose $T_m = 349.11\,^{\circ}\mathrm{C}$ is found and an average weight loss, including all heating rate, as 90.3 ± 2.2%. These values are close to that reported in the literature [23,24] where T_m values for cellulose is ~350 °C and the residue yield inferior to 10%.

The TG curve for alkali and earth alkaline salts of CMC are very similar regarding the shape, except the T_m value, which is characteristic for each sample. For $\beta = 10\,^{\circ}\mathrm{C\,min^{-1}}$, the T_m values and the average weight losses in parentheses, were: CMCLi = 294.14 (25.8 ± 0.7); CMCNa = 280.89 (45.0 ± 0.8); CMCK = 283.61 (42.0 ± 1.4); CMCMg = 319.03 (50.0 ± 1.1); CMCCa = 305.67 (48.7 ± 1.4); CMCBa = 295.14 (44.5 ± 1.0). The first relevant remark is that all of these CMC derivatives have T_m values lower than the parent cellulose (Fig. 5). In accordance with these data, the carboxymethylation decreases the thermal stability of cellulose. Second, T_m values for the earth alkaline salts of CMC are greater than that for the alkali one (Fig. 5). In such way, the earth alkaline salts of CMC are thermally more stable than the alkali counterpart. The reason for this behavior is probably due the divalent character of the earth alkaline counter-ion that may bond to more than one carboxylate anion, providing additional stabilization. Other periodic properties noted here is that the greater the ionic radius, the lower the thermal stability for a specific group alkali or earth alkaline salts (Fig. 5).

The CMC salts with transition metals as counter-ions showed lower stability considering the T_m value (Fig. 5) and a complex multi steps degradation pattern (Fig. 4). From the TG curves ($\beta = 10\,^{\circ}\mathrm{C\,min^{-1}}$) the following T_m and average weight loss in parentheses were found for CMCAl: $T_{m1} = 197.53$; $T_{m2} = 272.19$; $T_{m3} = 397.18$ (43.4 ± 0.8); CMCFe = $T_{m1} = 246.34$; $T_{m2} = 319.84$; $T_{m3} = 440.36$; $T_{m4} = 456.87$ (38.3 ± 0.5); CMCCu: $T_{m1} = 230.30$; $T_{m2} = 368.70$ (44.1 ± 0.1); CMCZn = $T_{m1} = 225.28$; $T_{m2} = 280.25$; $T_{m3} = 327.23$ (36.9 ± 1.0). This lower thermal stability of transition metal salts for the CMC, specially CMCFe and CMCCu, when compared to CMCNa, was reported earlier [25] and the reason for this multi steps degradation may relay to the formation of a complex-like structure involving metallic cations, carboxylate anions and water. The influence of cation in pyrolysis process is well known for cellulose [26] and the trend appears to be related to the size of the cation [27].

The thermal stability of the CMC is strongly influenced by the initial solution pH before precipitation. A sample of CMCNa recovered from an acid medium (pH 2.0 in HCl) showed a TG curve very different from a CMCNa sample recovered from an alkaline one (pH 12.0 in NaOH), as seen in Fig. 6. In this case the degree of ionization has an important role in the stabilization of the CMC. In acid condition some carboxylate groups are in the non-dissociate form, which

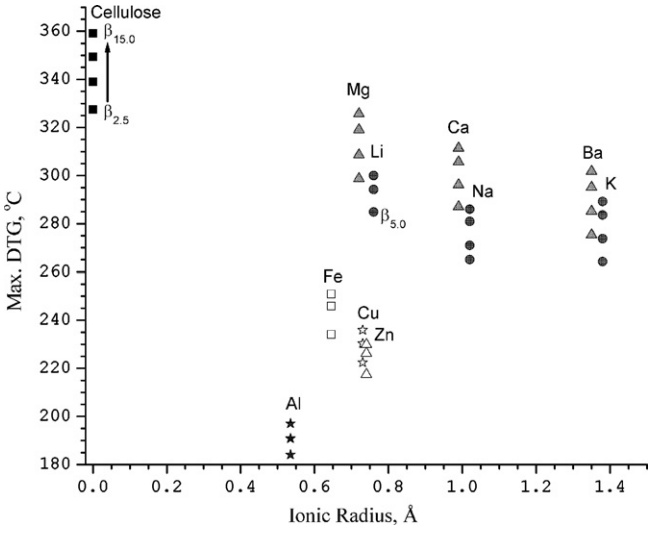

Fig. 5. T_m values from DTG curves plotted against the ionic radius of the counter-ion of CMC salts. Only for comparison, the cellulose was taken as "0". For the same sample, each point corresponds to different scan rates depicted as β_i.

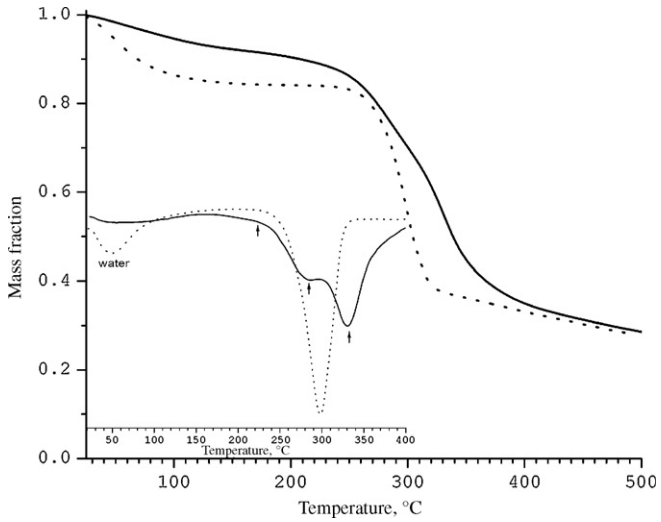

Fig. 6. TG curves from room temperature to 500 °C in nitrogen atmosphere for CMCNa recovered from an acid (—) and an alkaline (...) media at heating rate $\beta = 15.0\,^{\circ}\mathrm{C\,min^{-1}}$.

is noticeably less stable than the dissociated form. This finding confirms that intermolecular forces acting between the cation and the anion dictated the thermal stability of the CMC polyelectrolyte. This different degree of ionization may also affect the degree of humidity uptake.

3.4. Kinetic analysis of the TG curves

3.4.1. Theoretical background

The kinetic analysis of a thermal degradation process begins by expressing the reaction rate by a general equation such as:

$$\frac{d\alpha}{dt} = k(T)f(\alpha) \tag{1}$$

where t is the time, α is the extent of reaction, T is the temperature, $k(T)$ is the temperature-dependent rate constant and $f(\alpha)$ is a temperature-independent function that represents the reaction model. The rate constant $k(T)$ is given, generally, by the Arrhenius equation:

$$k(T) = A\exp\left(-\frac{E_a}{RT}\right) \tag{2}$$

where A is the pre-exponential or frequency factor and E_a is the apparent activation energy. Thus, Eq. (1) may be rewritten as:

$$\frac{d\alpha}{dt} = A\exp\left(-\frac{E_a}{RT}\right) \tag{3}$$

If the temperature is changed with the time ($\beta = dT/dt$) as it occurs in dynamic experiments, Eq. (3) assumes the form:

$$\frac{d\alpha}{dT} = \frac{A}{\beta}\exp\left(-\frac{E_a}{RT}\right) f(\alpha) \tag{4}$$

which, by integration results in:

$$g(\alpha) = \frac{A}{B}\int_o^T \exp\left(-\frac{E_a}{RT}\right) dT = \frac{A}{\beta} I(E_a, T) \tag{5}$$

where $g(\alpha)$ results from the integration of $f(\alpha)$.

Eqs. (3) and (5) are the fundamental expressions of analytical methods used to calculate the kinetic parameters on the basis of TGA data, applied to isothermal and isoconversional experiments. Some of the most common analytical expressions used to solve these equations and to find both E_a and A values are summarized in Table 2. These mathematical expressions were previously used in studies with cellulose [28] and other materials [29,30].

Once the apparent activation energy has been determined, it is possible to find the kinetic model which corresponds to a better description of the experimental data issued from the TG experiments. For this purpose, it is possible to define two especial functions which can easily be obtained by transformation of the experimental data, as proposed by Málek et al. [36,37]. For isothermal experiments these functions are:

$$Z(\alpha) = \left(\frac{d\alpha}{dt}\right) t \approx f(\alpha)g(\alpha) \tag{6}$$

$$Y(\alpha) = \left(\frac{d\alpha}{dt}\right) = f(\alpha) \tag{7}$$

The value of α at the maximum of the $Z(\alpha)$, α_Z^*, is characteristic of the kinetic model, the shape of the $Y(\alpha)$ function is formally identical to the kinetic model $f(\alpha)$ and its maximum value is labeled as α_Y^*.

Similarly, for dynamic conditions these functions, which have the same mathematical properties as those for isothermal conditions, are defined as:

$$Z(\alpha) = \left(\frac{d\alpha}{dT}\right) T^2 \approx f(\alpha)g(\alpha) \tag{8}$$

$$Y(\alpha) = \left(\frac{d\alpha}{dT}\right)\exp\left(\frac{E_a}{RT}\right) \approx Af(\alpha) \tag{9}$$

3.4.2. Kinetic parameters E_a and A of the cellulose and CMC

The mathematical approach described above was applied in the isothermal and dynamic data of the parent sample and its derivative CMC to determine the role of the counter-ion in the E_a values and its effectiveness in predicting the thermal stability of such polymers (Fig. 7).

Table 2
Kinetic methods used in evaluating E_a and A.

Method	Expression	Plot	Refs.
MacCallum	$\frac{E_a}{RT} + \ln[g(\alpha)] - \ln A = \ln t$	$\ln t$ versus $1/T$	[31]
Broido	$\ln\left[\ln\left(\frac{1}{1-\alpha}\right)\right] = \frac{-E_a}{RT} + \ln\left[\left(\frac{R}{E_a}\right)\left(\frac{A}{\beta}\right)T_m^2\right]$	$\ln[\ln[1/(1-\alpha)]]$ versus $1/T$	[32]
Ozawa–Flynn–Wall	$\log\beta = \log\frac{AE_a}{g(\alpha)R} - 2.315\frac{0.4567E_a}{RT}$	$\log\beta$ against $1/T$	[33]
Kissinger	$\ln\frac{\beta}{T_m^2} = \left\{\ln\frac{AR}{E_a} + \ln\left[n(1-\alpha_p)^{n-1}\right]\right\} - \frac{E_a}{RT_m}$	$\ln\beta/T_m^2$ versus $1/T_m$	[34]
Vyazovkin	$\Omega = \sum_i^n \sum_{j\neq i}^i \frac{I(E_{a\alpha}, T_{\alpha,i})\beta_j}{I(E_{a\alpha}, T_{\alpha,j})\beta_i}$	Ω attains a minimum	[35]

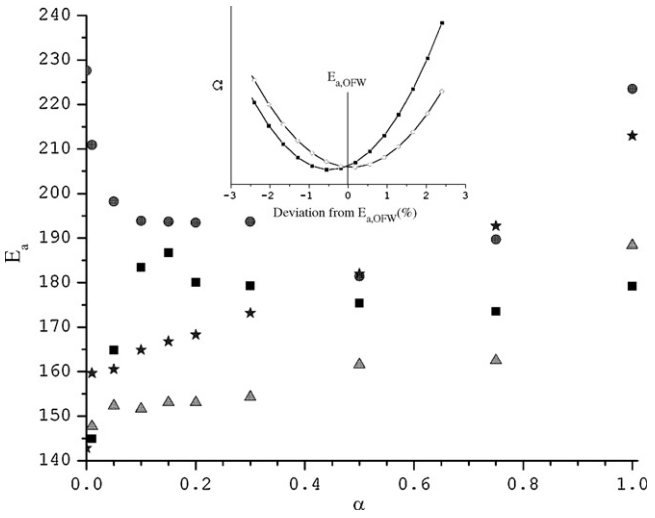

Fig. 7. E_a versus α dependency calculated according to Ozawa–Flynn–Wall method for cellulose (■); CMCNa (●); CMCK (▲); CMCCa (ξ). Vyazovkin method applied to cellulose for $\alpha(0.05)$ (■) and $\alpha(0.15)$ (○) is seen in the insert.

A critical examination of the mathematical approaches, mainly the single-rate-based one, applied to the dynamic experiments has given more credit and mechanistic significance to the isothermal experiments [31,38–40]. Consequently, the isothermal experiment was carried out with cellulose for comparison with the other approaches. The following E_a values were found, in kJ mol^{-1}, for each extent of reaction: $\alpha(0.025) = 130.7$; $\alpha(0.05) = 150.0$; $\alpha(0.10) = 164.8$; $\alpha(0.15) = 174.8$; $\alpha(0.20) = 184.5$; $\alpha(0.30) = 187.1$; excluding the first values the average was $E_a = 172.2 \pm 15$. This average E_a value is very close to that calculated by Kissinger and Ozawa–Flynn–Wall methods while Broido's values deviate from it (Table 3). Broido depicted his method studying the pyrolysis of the cellulose [32] and considered the reaction order as a first order process or $f(\alpha) = (1 - \alpha)$ based on a single heating rate measurement. In that study, Broido found $E_a = 55{,}000$ cal mol^{-1} (230 kJ mol^{-1}), a value that is very close to that calculated here for cellulose by this approach. Although this E_a value is probably over estimated due the first-order generalization and several approximations. In fact, other study reports [28] lower E_a values for cellulose in comparison with

Table 3
The Arrhenius parameters E_a and A, for the thermal degradation of cellulose and CMC determined according to Kissinger and Ozawa–Flynn–Wall.

Sample	Kissinger	Flynn–Wall–Ozawa	
	E_a (kJ mol^{-1})	E_a (kJ mol^{-1})[a]	A (min^{-1})[b]
Cellulose	172.2	181.0 ± 4.3	1.1×10^{15}
CMCLi	175.5	168.2 ± 1.6	4.2×10^{15}
CMCNa	213.1	194.6 ± 2.0	1.9×10^{18}
CMCK	170.10	152.9 ± 1.0	1.4×10^{14}
CMCMg	179.8	171.0 ± 6.0	1.2×10^{15}
CMCCa	190.8	166.7 ± 4.8	1.2×10^{15}
CMCBa	169.1	157.5 ± 3.3	2.1×10^{14}
CMCAl	–	133.4 ± 2.2	–
CMCCu	–	157.2 ± 6.8	–

[a] The average E_a was calculated for $0.05 \leq \alpha \leq 0.30$.
[b] The A values was calculated according to Ref. [30] assuming $\beta = 10\,^{\circ}$C min^{-1}.

the Broido's method. On the other hand, when $f(\alpha)$ is assumed to be a first order process for cellulose even other approaches gave high values for E_a close to 220 kJ mol^{-1} [26,41].

The isoconvertional method proposed by Ozawa–Flynn–Wall gives a more reasonable E_a values (Fig. 7). Furthermore, the E_a values calculated by this method are in very accordance with the values calculated by the new isoconvertional and more accurate method proposed by Vyazovkin. According to Vyazovkin's method, for a given set of experiments carried out at different heating rates, the activation energy can be determined at any particular extent of conversion by finding the value of E_a for which the function Ω attains a minimum [35]. Taking the E_a values calculated by the Ozawa–Flynn–Wall method as a first approximation and testing the dynamic data in the function Ω, a deviation smaller than 1% (Fig. 7) was observed for the E_a values. Such result was reported earlier [30] and shows the adequacy of the Ozawa–Flynn–Wall method to determine the E_a.

Now, the principal aim of this study is to compare the E_a values of different CMC salts to estimate their thermal stability. Unfortunately it was not possible to apply the mathematical treatment in all of the TG curves due to its complexity and multi step degradation pattern. The Kissinger E_a values (Table 3) do not show any periodicity as that seen for T_m in Fig. 5. On the other hand, the Ozawa–Flynn–Wall E_a values demonstrated a good relationship. Except for the high value of the CMCNa, all CMC salts have E_a inferior than that for cellulose. It is worth noting that E_a decreases

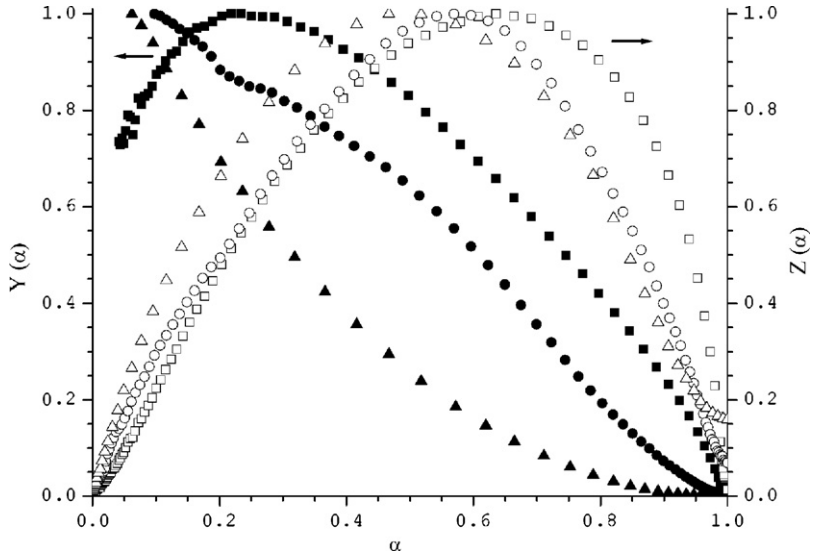

Fig. 8. Typical functions $Y(\alpha)$ (closed symbols) and $Z(\alpha)$ (open symbols) for the dynamic degradation ($\beta = 10.0\,^{\circ}$C min^{-1}) for the following samples: cellulose (■,□); CMCLi (●,○); CMCCa (▲,△).

Table 4
Kinetic parameters for cellulose and CMC salts determined according to Málek test for isothermal and dynamic TG data.

Sample[a]	Kinetic model	$f(\alpha)$	Parameters			
			α_Y^*	α_Z^*	m	n
Cellulose, β(2.5)	SB(n,m)	$\alpha^m(1-\alpha)^n$	0.26	0.598	0.38	1.09
Cellulose, β(5.0)			0.25	0.611	0.36	1.09
Cellulose, β(10.0)			0.23	0.664	0.28	0.91
Cellulose, β(15.0)			0.20	0.603	0.28	1.12
Cellulose isotherm T(290)			0.25	0.46	0.45	1.35
CMCLi	JMA(1)	$n(1-\alpha)[-\ln((1-\alpha)]^{1-(1/n)}$	0.00	0.569	–	1.0
CMCNa	SB(n,m)	$\alpha^m(1-\alpha)^n$	0.11	0.478	0.23	1.89
CMCK	SB(n,m)	$\alpha^m(1-\alpha)^n$	0.42	0.530	1.59	2.19
CMCMg	RO($n>1$)	$(1-\alpha)^n$	0.00	0.572	–	1.91
CMCCa	RO($n>1$)	$(1-\alpha)^n$	0.00	0.492	–	2.06
CMCBa	RO($n>1$)	$(1-\alpha)^n$	0.00	0.491	–	1.92

[a] Otherwise specified the $\beta = 10.0\,^{\circ}\mathrm{C\,min^{-1}}$.

as the atomic number for a specific group alkali or earth alkaline salts increases (Table 3). The high E_a value found for CMCNa salt do not have a reasonable explication, however, it was observed by the isothermal MacCallum approach as well ($E_a = 197.5 \pm 12$). For CMC salts of transition metals, the mathematical treatment becomes inappropriate due the imprecision in setting initial and final extents of reaction, α, mainly for the isoconversional Ozawa–Flynn–Wall method.

3.4.3. Further information about kinetic parameters of the cellulose and CMC

Further information can be obtained from the TG curve regarding the analytical expression that describes the kinetic model, $f(\alpha)$. Having in hands the E_a and A values, the most probable kinetic model can be determined and compared to the experimental curves. For this, the procedure proposed by Málek (Eqs. (6)–(9)) was used in the isothermal and dynamic experiments. Some typical $Z(\alpha)$ and $Y(\alpha)$ functions are shown in Fig. 8. The resulting $Z(\alpha)$ and $Y(\alpha)$ curves for cellulose, CMCNa and CMCK showed almost the same profile with $Y(\alpha)$ with a maxima such that $0 < \alpha_Y^* < \alpha_Z^*$. Thus, the catalytic SB(n,m) model proposed by Šesták [42] yields the best fit. Specifically for cellulose this kind of model was confirmed recently to be more appropriated in detriment of a first-order one [41]. CMCLi showed a very different profile with $Y(\alpha)$ having a maxima in $\alpha_Y^* = 0$ and steadily decreases linearly. Therefore, its degradation process can be satisfactory described by the Johnson–Mehl–Avrami model or JMA(1). The $Y(\alpha)$ for CMCMg, CMCCa and CMCBa decreases steadily, having its maxima at $\alpha_Y^* = 0$, although its shape is concave. Thus, the reaction order, RO ($n > 1$) is the most appropriated fitting model. Different isothermal temperatures or different scan rates do not influence in the shapes of the $Z(\alpha)$ and $Y(\alpha)$ functions, except for a small variation in their maxima. According to each kinetic model, the exponents m or n are determined, completing all needed parameters to plot a simulated curve (Table 4).

Thus, by substituting the values of E_a and A and the expression for $f(\alpha)$ in Eqs. (3) or (4), it is possible to simulate the curve $d\alpha/dt$ or $d\alpha/dT$ which, after normalization, may correspond to the experimental one. The simulated and the experimental curves corresponding to the thermal degradation of cellulose and CMC salts showed a good agreement in the range of α attained in our experiments (Fig. 9), indicating that the kinetic parameters and the expression of $f(\alpha)$ adopted for the simulation are quite suitable. The best fitted model was achieved for cellulose, CMCMg, CMCCa and CMCBa, which resulted in a lower residual difference between the curves, although the percentage difference for other cases was lower than 2% even for $\alpha < 0.2$ and $\alpha > 0.8$.

To define an exact kinetic model, this analysis shows that very similar materials behave significantly different in the pyrolysis and a very complex mathematical description [30] would require defining a satisfactory approach. Nevertheless, some insights on possible mechanisms of degradation can be depicted [30,42]. For instance, the parameters m and n in the SB model describe, respectively, the acceleration and deceleration of the decomposition rate with respect to the conversion. Thus, they describe the reaction that begins with an acceleration of the degradation rate until a maximum is attained, when an nth order-like deceleration becomes dominant through the reaction completion. Moreover, this suggests a process controlled by nucleation. On the other hand, the RO kinetic model may be related to a phase-boundary controlled processes. It is known, however, that complex degradation processes generally follow a kind of kinetic model in the earlier stage, changing to another in the later stages of degradation [42].

FTIR analysis can confirm the probable kinetic model described earlier. Thus, if the extent of the reaction, σ, is expressed as a function of the decrease on the absorbance for a given characteristic band in function of the time, then $\sigma = (A_0 - A_t)/A_0$, where A_0 is the absorbance of a given band at zero time and A_t is the absorbance of the same band at time t. Thus, the plot of $d\sigma/dt$ versus t must be closely similar to $d\alpha/dt$, i.e., the degradation kinetic model. Doing this for the bands at 1595 and 1417 $\mathrm{cm^{-1}}$, referent to degradation of the carboxylate anion, the plot $d\sigma/dt$ versus t (Fig. 10) does not show any maxima. Therefore, these degradation reactions are predominantly decelerative, hence better described by a kinetics model of the type $(1-\alpha)^n$. Conversely, as a maximum is observed in the curve due to the band of the glycosidic bond at 890 $\mathrm{cm^{-1}}$ and the carbonyl group C=O at 1740 $\mathrm{cm^{-1}}$ (Fig. 10), it can be attributed to an acceleratory phase followed by a deacceleratory one. Therefore the two

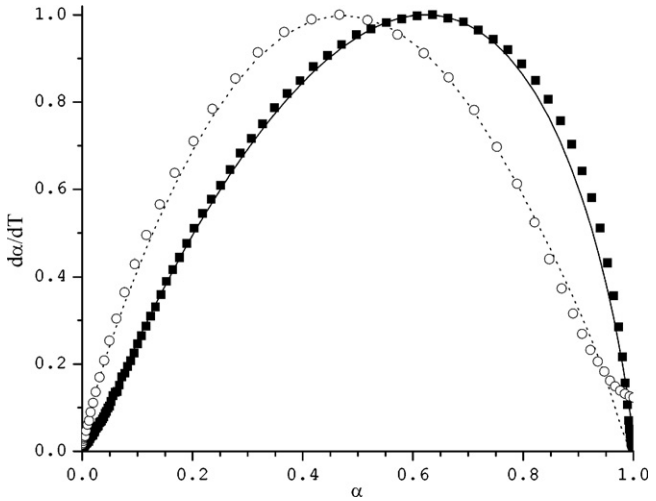

Fig. 9. Experimental (symbols) and simulated (lines) curves $d\alpha/dt$ versus α for the dynamic degradation ($\beta = 10\,^{\circ}\mathrm{C\,min^{-1}}$) for cellulose: (■,—) and CMCCa (○,…).

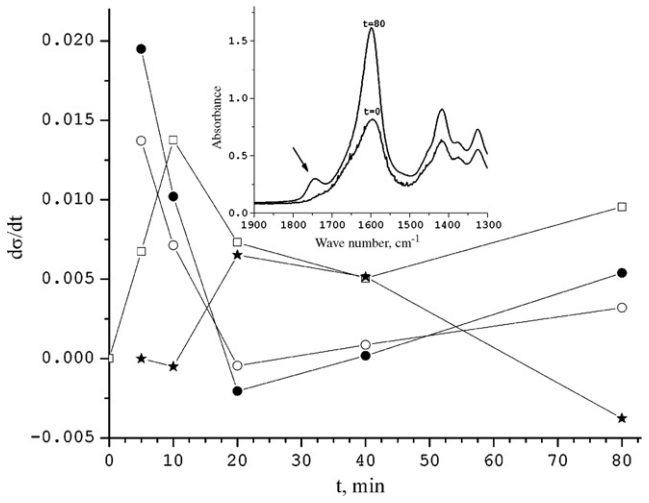

Fig. 10. Plot of $d\sigma/dt$ versus t for infrared bands due to vibrations of C=O (□ = 1740 cm^{-1}), carboxylate anion (● = 1595 cm^{-1}, ○ = 1417 cm^{-1}), and glycosidic bond (ξ = 890 cm^{-1}). The FTIR spectra in the range 1300–1900 cm^{-1} of films of CMCNa degraded for 0 and 80 min at 220 °C are seen in the insert.

parameters SB model seems to be more suitable. This kind of behavior has been reported for chitosan that has a very similar backbone constitution [30].

Another very important finding in the FTIR degradation study was the appearance of a band at 1740 cm^{-1} that increases steadily with the degradation time (see the insert in Fig. 10). A band at this frequency is characteristic of the axial deformation of the carbonyl group C=O, although only when belonging to a non-dissociated acid or ester group [43]. This makes clear that an intermediary acid or ester compound involving the carboxylate group is formed during the early step of degradation. The formation of such compound shows a predominantly acceleratory behavior (Fig. 10).

4. Conclusions

Polyelectrolyte like CMC is a very interesting class of polymers that exhibit special properties in solution or in solid-state conditions. Furthermore, these properties can be entirely different by just changing the counter-ions as effectively observed by the degree of humidity and the thermal stability. Special care must be taken when CMC is used in the solid-state in combination with other chemicals, where the presence of cations can lead the CMC to present unexpected properties. Another important remark in this study is that only the kinetic parameters are not enough to predict the thermal stability of the CMC salts. Such parameters must be interpreted in association with the temperature of maximum degradation rate that showed a remarkable periodic property. For less complex TG curves, the Ozawa–Flynn–Wall method provided good results. FTIR analysis showed to be useful in elucidating the kinetic model and providing information about intermediary compounds formed during thermal degradation.

Acknowledgements

The authors are grateful to Dr. Luis C. Morais for the donation of the cellulose pulp and to FAPESP, Embrapa and CNPq for financial support.

References

[1] J.-L. Ren, R.-C. Sun, F. Peng, Polym. Degrad. Stab. 93 (2008) 786–793.
[2] T. Heinze, A. Koschella, Macromol. Symp. 223 (2005) 13–39.
[3] http://www.food.gov.uk/safereating/chemsafe/additivesbranch/enumberlist accessed in January, 2009.
[4] J.B. Batdorf, J.M. Rossman, in: R.L. Whistler (Ed.), Sodium Carboxymethylcellulose, Academic Press, New York, 1973.
[5] E. Ott, H.M. Spurlin, M.W. Graffin, Cellulose and Cellulose Derivatives, Interscience Publisher, New York, 1954.
[6] U. Käistner, H. Hoffmann, R. Dönges, J. Hilbig, Colloids Surf. A 123 (1997) 307–328.
[7] B. Porsch, B. Wittgren, Carbohydr. Polym. 59 (2005) 27–35.
[8] X.H. Yang, W.L. Zhu, Cellulose 14 (2007) 409–417.
[9] G.D. Machado, A.M. Regiani, A. Pawlicka, Polimery 48 (2003) 273–279.
[10] T. Heinze, H. Winkelmann, D. Klemm, Acta Polym. 41 (1990) 76–81.
[11] D.S. Ruzene, A.R. Goncalves, J.A. Teixeira, M.T.P. De Amorim, Appl. Biochem. Biotechnol. 137 (2007) 573–582.
[12] P. Khristova, O. Kordsachia, R. Patt, I. Karar, T. Khider, Ind. Crops Prod. 23 (2006) 131–139.
[13] D. Fengel, G. Wegener, Wood: Chemistry, Ultrastructure, Reactions, Walter de Gruyter, Berlin–New York, 1984.
[14] W.H. McMaster, N. Kerr Del Grande, J.H. Mallett, J.H. Hubbell, Lawrence Livermore National Laboratory Report, Argonne, 1969.
[15] D.L. VanderHart, R.H. Atalla, Macromolecules 17 (1984) 1465–1472.
[16] D. Capitani, M.A. Del Nobile, G. Mesintieri, A. Sannino, A.L. Segre, Macromolecules 33 (2000) 430–437.
[17] D. Capitani, F. Porro, A.L. Segre, Carbohydr. Polym. 42 (2000) 280–286.
[18] J. Berthold, J. Desbrieres, M. Rinaudo, L. Salmen, Polymer 35 (1994) 5729–5736.
[19] J. Berthold, R.J.O. Olsson, L. Salmen, Cellulose 5 (1998) 281–298.
[20] C. Fringant, J. Desbrieres, M. Milas, M. Rinaudo, C. Joly, M. Escoubes, Int. J. Biol. Macromol. 18 (1996) 281–286.
[21] H.P. Yang, R. Yan, H.P. Chen, D.H. Lee, C.G. Zheng, Fuel 86 (2007) 1781–1788.
[22] R.J. Evans, T.A. Milne, Energy Fuels 1 (1987) 123–137.
[23] N. Shimada, H. Kawamoto, S. Saka, J. Anal. Appl. Pyrol. 81 (2008) 80–87.
[24] S. Soares, G. Camino, S. Levchik, Polym. Degrad. Stab. 49 (1995) 275–283.
[25] M.P. Prasad, M. Kalynasundaran, J. Appl. Polym. Sci. 54 (1994) 1879–1885.
[26] M.J. Antal Jr., G. Várhegyi, Ind. Eng. Chem. Res. 34 (1995) 703–717.
[27] M.R. Nimlos, S.J. Blanksby, G.B. Ellison, R.J. Evans, J. Anal. Appl. Pyrol. 66 (2003) 3–27.
[28] F. Yao, Q. Wu, Y. Lei, W. Guo, Y. Xu, Polym. Degrad. Stab. 93 (2008) 90–98.
[29] D. Britto, S.P. Campana-Filho, Polym. Degrad. Stab. 84 (2004) 353–361.
[30] D. Britto, S.P. Campana-Filho, Thermochim. Acta 465 (2007) 73–82.
[31] R. MacCallum, in: C. Booth, C. Price (Eds.), Thermogravimetric Analysis, Pergamon Press, Oxford, 1989.
[32] A. Broido, J. Polym. Sci. A 27 (10PA) (1969) 1761–1773.
[33] T. Ozawa, J. Therm. Anal. Calorim. 2 (1970) 301–324.
[34] H.E. Kissinger, Anal. Chem. 29 (1957) 1702–1706.
[35] S. Vyazovkin, D. Dollimore, J. Chem. Inf. Comput. Sci. 36 (1996) 42–45.
[36] J. Málek, J. Šesták, F. Rouquerol, J.M. Criado, A. Ortega, J. Therm. Anal. 38 (1992) 71–87.
[37] S. Montserrat, J. Málek, P. Colomer, Thermochim. Acta 313 (1998) 83–95.
[38] A.K. Galwey, Thermochim. Acta 407 (2003) 93–103.
[39] S. Vyazovkin, C.A. Wight, Thermochim. Acta 340–341 (1999) 53–68.
[40] M.E. Brown, M. Maciejewski, S. Vyazovkin, R. Nomen, J. Sempere, A. Burnham, J. Opfermann, R. Strey, H.L. Anderson, A. Kemmler, R. Keuleers, J. Janssens, H.O. Desseyn, C.-R. Li, T.B. Tang, B. Roduit, J. Málek, T. Mitsuhashi, Thermochim. Acta 355 (2000) 125–143.
[41] R. Capart, L. Khezami, A.K. Burnham, Thermochim. Acta 417 (2004) 79–89.
[42] J. Šesták, G. Berggren, Thermochim. Acta 3 (1971) 1–12.
[43] K. Pal, A.K. Banthia, D.K. Majumdar, Biomed. Mater. 1 (2006) 85–91.